High-energy excitonic effects in single-layer graphene

Eri Widianto[1,2], Lucky Zaehir Maulana[3], Edi Suharyadi[2], Angelo Giglia[4],

Konstantin Koshmak[4], Stefano Nannarone[4], Andrivo Rusydi[5,6,†], Iman Santoso[2,*]

[1]*Department of Mechanical Engineering, Faculty of Engineering, Universitas Singaperbangsa Karawang, Telukjambe Timur, Karawang 41361, Indonesia.*

[2]*Department of Physics, Faculty of Mathematics and Natural Sciences, Universitas Gadjah Mada, Sekip Utara PO Box BLS 21, Yogyakarta 55281, Indonesia.*

[3]*Department of Physics, Faculty of Science and Technology, Universitas Jambi, 36361, Indonesia.*

[4]*CNR-Istituto Officina Materiali, I-34149 Trieste, Italy.*

[5] *Advanced Research Initiative for Correlated-Electron Systems (ARiCES), Department of Physics, National University of Singapore, 2 Science Drive 3, Singapore 117551, Singapore.*

[6] *Singapore Synchrotron Light Source, 5 Research Link, Singapore 117603, Singapore.*

E-mail: * iman.santoso@ugm.ac.id and † andrivo.rusydi@nus.edu.sg

Using high-energy polarization-dependent reflectivity, we discover concomitantly novel high energy (soft X-ray) two-dimensional correlated-plasmons with extremely low-plasmonic-loss and high optical energy resonant excitons at room temperature in graphene. The high-energy correlated-plasmons strongly depend on the photon polarizations, i.e. at ~23.7 eV and ~37.3 eV for p- and s-polarized photons, respectively. The resonant excitons occur at ~10.04 eV and ~12.29 eV arising from transitions between parallel σ and π^* states along $\Gamma - K$, as well as σ and σ^* states at M point, respectively. The observation of spectral weight transfer signifies electronic corelation and that the two-dimensional nature and low-energy properties are strongly coupled with high-energy bands. Our result shows the importance of electron-electron and electron-hole interactions in determining electronic and optical properties of graphene and two-dimensional systems.

Electronic correlation is believed to play important role in determining exotic properties, such as high-Tc superconductivity and colossal magneto resistance, in two-dimensional (2D) and

strongly correlated electron systems in general. Photons of high optical energies are the key to probe electronic correlation [1–4]. Of particular interest is to understand electronic correlation and the origin of 2D nature properties in graphene. Graphene, since it was discovered in 2004, has generated significant attention in the global research community due to its exotic quantum properties. The sp^2 hybridized carbon atoms form a one-atom-thick honeycomb structure, and its electrons and holes follow the 2D Dirac equation, exhibiting an unusual linear dispersion band structure at the K-point of the Brillouin zone [5,6]. The investigation of electron-electron ($e-e$) and electron-hole ($e-h$) systems is crucial for exploring many-body quantum phenomena such as unconventional, correlated plasmons and high-energy excitons [4,7–9]. While correlated plasmons are collective quantum oscillations of correlated charges, high energy excitons have composed of an electron and a hole in high energy bands. They both are dominating the optical response of correlated electron systems affecting their binding, relaxation processes and other physical properties [10]. While the investigation of high-energy excitons and electronic correlation in graphene remain hotly discussions, thus far there is no report on high-energy *two-dimensional* correlated plasmons in graphene [11,12] (see Table S1 in Ref. [13]).

Theoretical studies using the *ab initio* many-body perturbation based on the GW approximation and Bethe–Salpeter equation (BSE) approach have predicted and emphasized the significance of electronic correlation resulting in resonant excitonic phenomena in the optical absorption of graphene [14,15]. Theoretical calculations have predicted resonant excitonic effects in which depending on the correlation effect, their excited states could generate a series of resonant excitons due to the unique band structures in graphene [14–17]. Experimentally, resonant exciton at 4.6 eV has been observed and attributed to ($e-h$) interaction in the π and π^* bands at the M-point [18–28]. These effects were observed in broadly resonant excitonic states comprising π and

π^* bands within the low-energy range (<10 eV), with short lifetimes and no binding energy. However, it remains a discrepancy with regard to optical properties beyond 10 eV [11,15,17], which require to reveal electronic correlation.

Theoretical calculations at the higher-energy range have suggested that if many-body correlations are involved, then graphene generally would have predicted to generate high-energy resonant excitonic effects even up to ~20 eV [17]. Importantly, many-body effects connect between high-energy bands and low-energy properties [1,2]. The role of electronic correlations, i.e., electron-electron ($e-e$) and electron-hole ($e-h$) interactions, in graphene and 2D systems in general remains hotly debated [14,15,17]. Based on theoretical and recent experimental studies, high-energy optical properties are the key to distinguishing correlation effects in graphene [17] and 2D systems [4]. Until now, there has been no systematic experimental study of high-energy optical properties of free-standing or suspended graphene.

Furthermore, previous optical measurements were frequently conducted on isolated free-standing graphene, which is usually very tiny and thus needs extensive experimental [23–29]. Our study aims to fill this gap by investigating the optical properties of CVD graphene, which is produced using a low-cost method that is compatible with chip fabrication and can yield large-area samples up to 100 m long [30]. By studying the high-energy optical properties of graphene, we hope to address the outstanding, fundamental problem on electronic correlation and improve our understanding of its electronic structure and potential applications. Moreover, the ability to regulate the polarization-dependent optical response of graphene is crucial for controlling the interaction between graphene and light, which is essential for the progress of novel optoelectronic devices based on graphene. Modifying the polarization of light allows for the targeted stimulation

of various electronic states in graphene, as well as regulation of the material's absorption, transmission, and reflection of light [31–39].

In this Letter, we report novel high energy (soft X-ray) correlated-plasmons with extremely low-plasmonic-loss and high optical energy resonant excitons due to many-body correlation effects in single-layer CVD graphene on SiO_2/Si substrate. Due to weak interaction with the substrate, the single-layer CVD graphene is free standing-*like* [18,26,28] and, supported with theoretical calculations, these novel optical properties are the 2D nature of graphene. The free standing-*like* graphene is different than previous studies where graphene-substrate interactions have been found to play fundamental roles in modifying the optical response and electronic interactions of graphene [28,40–46]. The nature of the interface contributes to the carrier density and work function of graphene, which are fundamental properties for optoelectronics devices [47,48]. Therefore, it is crucial to investigate free standing graphene or weakly graphene-substrate interaction. We examine, *for the first time*, the polarization-dependent complex dielectric function and loss function of single layer graphene within the 9-40 eV energy range. Surprisingly, the high-energy correlated-plasmons and high-energy resonant excitonic effects show strong polarization between s- and p-polarization. The existence of high-energy resonant excitons and correlated plasmons reveals the importance of $e-e$ and $e-h$ interactions in free standing graphene and the low-energy bands are tightly connected with high-energy bands. This implies that one has to understand and treat graphene as a correlated system rather than that of a non- or weakly correlated system. Our measurements use single-layer graphene on SiO_2 (~285 nm)/Si substrate purchased from Graphene Laboratories Inc, Graphene Supermarket, US. The optical reflectivity of single-layer graphene was measured using a vacuum ultraviolet (VUV) reflectivity at IOM-CNR synchrotron beamline BEAR (Bending magnet for Emission Absorption and Reflectivity) at

Elettra (Trieste, Italy) using s- and p-polarized light with the near-normal incident angle of 15° [49].

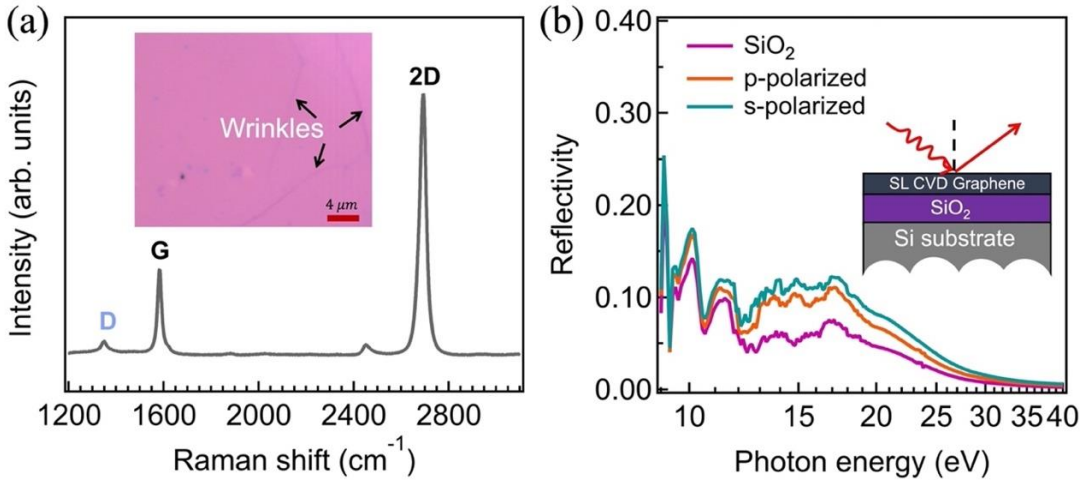

FIG. 1. (a) Raman shift of single-layer graphene. The inset shows an optical micrograph of single-layer graphene with some wrinkles. (b) Reflectivity measurements (s- and p-polarized) of graphene and SiO_2/Si substrate. Inset: A sketch shows the optical model of the reflectivity experiment at high energy (9–40 eV).

Figure 1 (a) shows the optical micrograph and Raman shift of single-layer graphene. The Raman spectra of graphene reveal the characteristic G and 2D bands at 1581 cm^{-1} and 2692 cm^{-1}, respectively, with weak peak-related defect (D band) also present at 1346 cm^{-1}. The ratio of the intensities of the 2D to G bands (I_{2D}/I_G) is approximately two, and the 2D band exhibits a symmetric single Lorentzian shape, confirming the presence of single-layer graphene in our sample. Figure 1 (b) presents the measured reflectivity of each sample. The fitted reflectivity of each sample is matched closely to its respective measured reflectivity (see Fig. S1 in Ref. [13]). Our significant finding is the high-energy reflectivity observed in single-layer graphene, particularly at s- and p-polarizations, compared to the SiO_2/Si substrate, as illustrated in Fig. 1 (b). The reflectivity of graphene is found to be polarization-dependent and is significantly higher than

that of SiO_2. Significant differences in reflectivity exist between the substrate and graphene samples, particularly at high photon energy ranges of 9–40 eV.

The procedure for obtaining the complex dielectric constant ($\tilde{\varepsilon} = \varepsilon_1 + i\varepsilon_2$) of single-layer graphene involves modeling the sample with Fresnel coefficients for an optical multi-layered film (see Fig. S2), following the approach described in Ref. [50,51]. While previous experimental studies [52,53] have identified resonant excitonic effects within the photon energy range of up to ~8 eV, our study reveals new excitonic effects well above it. The real ε_1 (Fig. 2a) and imaginary ε_2 (Fig. 2b) parts of the dielectric function of single-layer graphene show a strong polarization dependence. We reveal two types of excitonic effects: (i) a broad, widely resonant excitonic that reshapes the single-particle interband absorption peak but do not shift the absorption edge, and (ii) a sharp resonant exciton below the continuum. Both types of excitons have comparable optical absorption, resulting in a unique double-peak characteristic that is consistent with previous theoretical predictions [17]. These two excitonic states have energies of approximately ~10.04 eV and ~12.29 eV, respectively, and correspond to transitions between parallel σ and π^* states and σ and σ^* states, as shown in the band structure of free-standing graphene in Ref. [17].

We compare our experimental data with first-principle calculations of optical absorbance reported in Ref. [17] to determine the origin of both peak excitons. The inset graph in Fig. 2 (b) shows that the optical absorption spectra of graphene exhibit a significant peak around 12 to 20 eV related to the nearly parallel σ and π^* states and their high joint density of states (JDOS), without $e-h$ interactions. The peak is broadened since these bands are not exactly parallel. Interestingly, the optical absorption spectra of graphene change dramatically accompanied with spectral weight transfer in a broad energy range even well above 20 eV when $e-e$ and $e-h$ interactions are included, resulting in two optically bright excited states: the prominent exciton

with an energy of approximately ~12.54 eV and a widely resonant excitonic state with an energy of around ~13.75 eV, while the interband transitions above ~15 eV are dramatically suppressed [17]. Remarkably, as shown in Fig. 2 (b), the line shape between our experimental data and the first-principle calculations from Ref. [17] is very similar, providing conclusive evidence of the 2D nature of resonant excitons due to strong $e-e$ and $e-h$ interactions in graphene.

Our other significant observation is novel high-energy correlated plasmons seen in the loss function, LF (Fig. 2 (c)). The LF is calculated using $\mathrm{LF}(\omega) = -\mathrm{Im}[\tilde{\varepsilon}^{-1}(\omega)] = \varepsilon_2(\omega)/\varepsilon_1^2(\omega) + \varepsilon_2^2(\omega)$. For sub-X-ray photons, the photon momentum transfer, q, is finite but approaches zero, and the distinction between longitudinal (*l*) and transverse (*t*) $\varepsilon(\omega)$ vanishes, that is, $\lim_{|\mathbf{q}|\to 0} \varepsilon_l(\mathbf{q},\omega) = \varepsilon_t(\mathbf{q},\omega)$, allowing to probe both optical and plasmonic properties in the low-q limit [4,9]. The high-energy correlated plasmons can be identified as follows: (i) a peak in LF, (ii) a positive, smaller value (nearly zero) of ε_1, (iii) a peak shift in ε_2, if any, and (iv) a local minimum in reflectivity [9]. For soft X-ray where multiple excitations occur, instead reflectivity shows a decreasing in monotonic fashion, which also can have local minimum [4,54]. The LF peaks at ~23.7 eV and ~37.3 eV fulfil all these criteria, i.e. extremely low-loss ε_2 at ~23.7 eV and ~37.3 eV is 0.33 and 0.03 (Fig. 1(a)), respectively, ε_1 at ~23.7 eV and ~37.3 eV is 0.027 and 0.003 (Fig. 1(b)), respectively, and a decreasing reflectivity in a monotonic fashion (see Fig. S4 in Ref. [13]). Correlated plasmons arise in materials where electron correlation significantly impact the collective behavior of charge carriers, which manifest in a smaller value (nearly zero but remains positive) of ε_1, while for the conventional plasmon, one expected the crossing of ε_1 to the energy axis [4]. By assuming a free electron gas, the equation for plasma frequency applies $\omega_\mathrm{p} = {}^{E_\mathrm{p}}/_{\hbar} = \sqrt{\frac{ne^2}{m_e\varepsilon_0}}$, where n is the electron density, m_e is the electron mass, ε_0 is the permittivity of free space,

e is the elementary charge, $\hbar$ is the reduced Planck's constant, and ω_p and $E_p$are the plasmon frequency and energy, respectively. In conventional terms, the ~23.7 eV plasmon would have an electron density of 3.25×10^{22} cm^{-3}. For the ~37.3 eV plasmon has an electron density of 8.04×10^{22} cm^{-3}. These values are clearly not feasible and further support that these high-energy correlated-plasmons are quantum oscillations of correlated-charges.

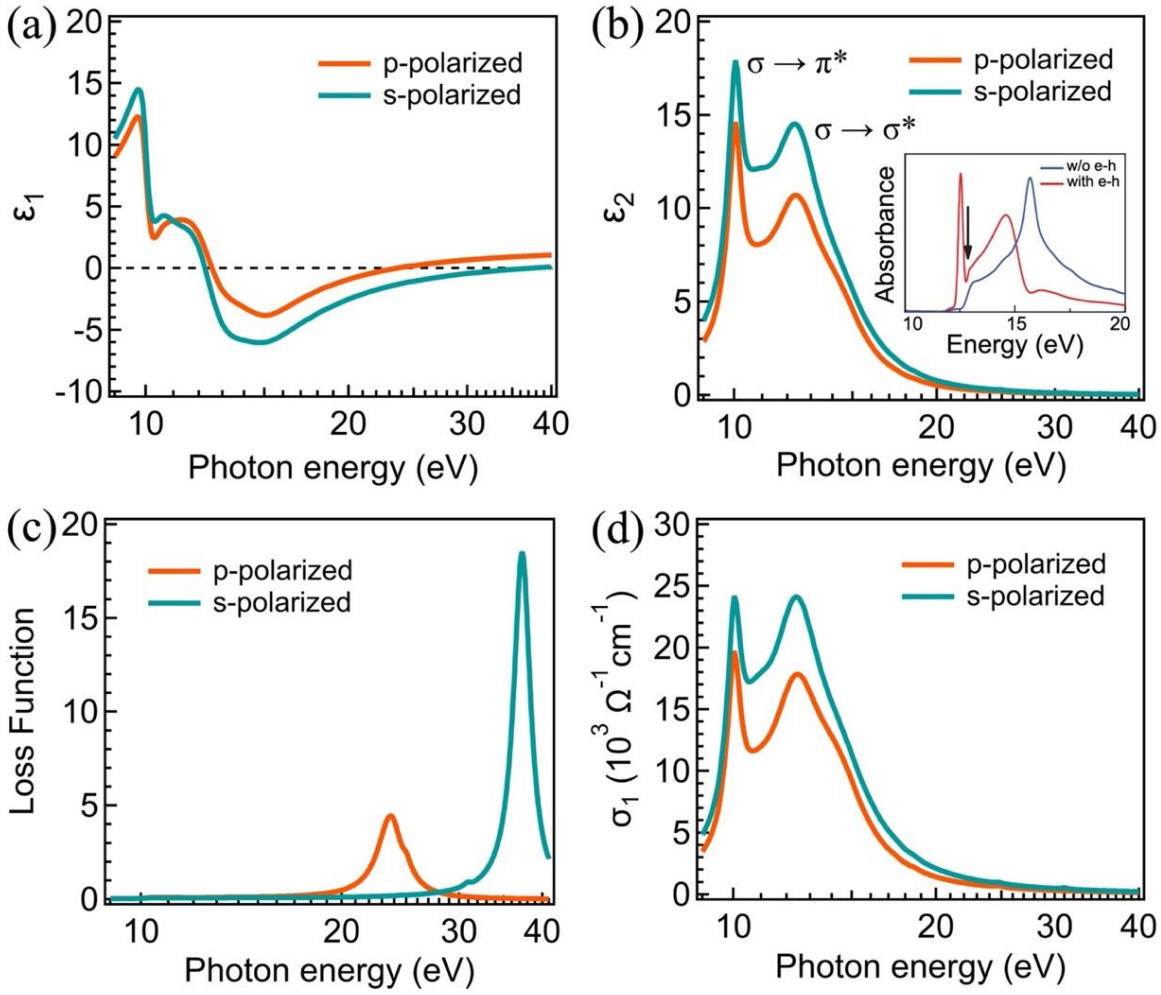

FIG. 2. Experimental polarization-dependent measurement of single-layer graphene: (a) The real part of the dielectric constant (ε_1). (b) The imaginary part of the dielectric constant (ε_2). The inset shows optical absorption spectra with and without $e-h$ interaction of graphene using first-principles calculations from ref. [17]. (c) The loss function (d) The real part of the optical conductivity (σ_1).

The optical conductivity (σ_1) of single-layer graphene as a function of the imaginary part (or absorption) of the complex dielectric constant (ε_2) by the equation: $\sigma_1 = \omega\varepsilon_2/4\pi$ is depicted in Fig. 2 (d). Figure 2 demonstrates that the optical absorption of graphene is highly influenced by the polarization of the incident light. Generally, the absorption and scattering of s-polarized light are greater than those of p-polarized light. The electronic bands in graphene exhibit high anisotropy, meaning that they possess different properties in different directions. When, on the one hand, linearly polarized light with its electric field vector parallel to the graphene plane (s-polarization) is incident on graphene, the response is mainly from the σ-electron of graphene, which is a linear combination of the s-p_x and s-p_y orbitals. On the other hand, when linearly polarized light with its electric field vector perpendicular to the graphene plane (p-polarization) is incident on graphene, the response is primarily from the π-electron of graphene, which comes from p_z orbital of carbon atoms. Due to a finite incident angle, the incoming electric field vector for this polarization is reduced. Therefore, this could lead to the smaller differences between s and p reflectivity observed in our data because there is no reducing electric field vector for s-polarization.

Theoretical calculations based on DFT have been used to investigate graphene on bare Si substrate [55]. When positioned near Si (111) and (100) surfaces, carbon atoms in graphene can form covalent interactions with Si atoms. On the Si (111) surface, the Fermi level of graphene shifts, leading to a three-orders-of-magnitude increase in electron density. The work function of graphene on this surface also increases by 0.29 eV, likely due to the surface dipole caused by the redistribution of π orbitals. The interaction between graphene and the Si surface modifies the number of available states below the Fermi level, resulting in significant changes in electron density and work function [55]. The remarkable rise in charge density observed is attributed to an unconventional n-type doping mechanism, which modifies the DOS instead of transferring

charges. The shift of the Fermi level towards the conduction band is higher than both the Dirac point of graphene and the top of the valence band of Si. One possible explanation is that the interaction between the graphene and Si surface reduces the number of available states of both graphene and Si below the Dirac point [55].

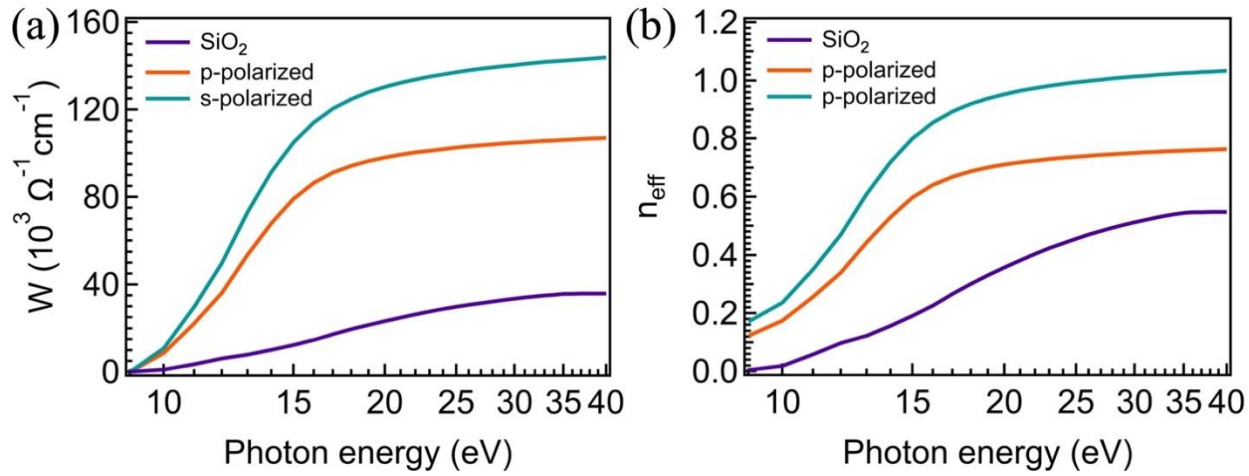

FIG. 3. (a) Spectral weight transfer and (b) The amount of charge redistribution of single-layer graphene on SiO_2

The effect of the substrate on the resonant exciton properties of single-layer graphene on SiO_2/Si substrates is evaluated by looking at their respective spectral weight (W). Figure 3(a-b) depicts the spectral weight analysis of graphene compared with SiO_2 in the area related to the change of the absorption features. The spectral weight: $W = \int_{E1}^{E2} \sigma_1 dE$ is derived for finite energy ranges to estimate the transfer of charge carriers for different energy regions. At an energy range of 9-15 eV, whereas resonant excitons occur, W for graphene is much bigger than that of W for SiO_2, revealing that the large spectral weight is from graphene and further supporting for the important role of electronic correlations. There might be a local bonding between substrate and graphene, which may cause a shift of the resonant exciton peaks [11,55]; however, electronic correlations remain dominant. It is worth noting that the optical properties of single-layer graphene

are different than that of epitaxial graphene on a 6H-SiC(0001)/buffer layer, which is not a free standing graphene and has high-energy resonant exciton at ~6.3 eV [11]. While, the optical properties of graphene on quartz are much closer to the theoretical calculations based on GW-BSE [17]. This strongly suggests that the quartz substrate has less effect on the optical properties of graphene, making it free standing-*like* graphene.

Figure 4 (a-b) shows the decomposition of the room-temperature universal optical conductivity ($\pi e^2/2h$) of single-layer graphene for s- and p-polarizations. We fit the optical conductivity spectra with the Lorentz model (blue), which can be associated with interband transition and two Fano-shaped vibration modes (purple and green). The Fano line shape indicates coupling (or resonance) between a discrete state and a continuum of electronic states within the same energy range [52,56]. In our case, this coupling occurs between a discrete excitonic state, resulting from e-h interactions, and a continuum of the electronic band structure.

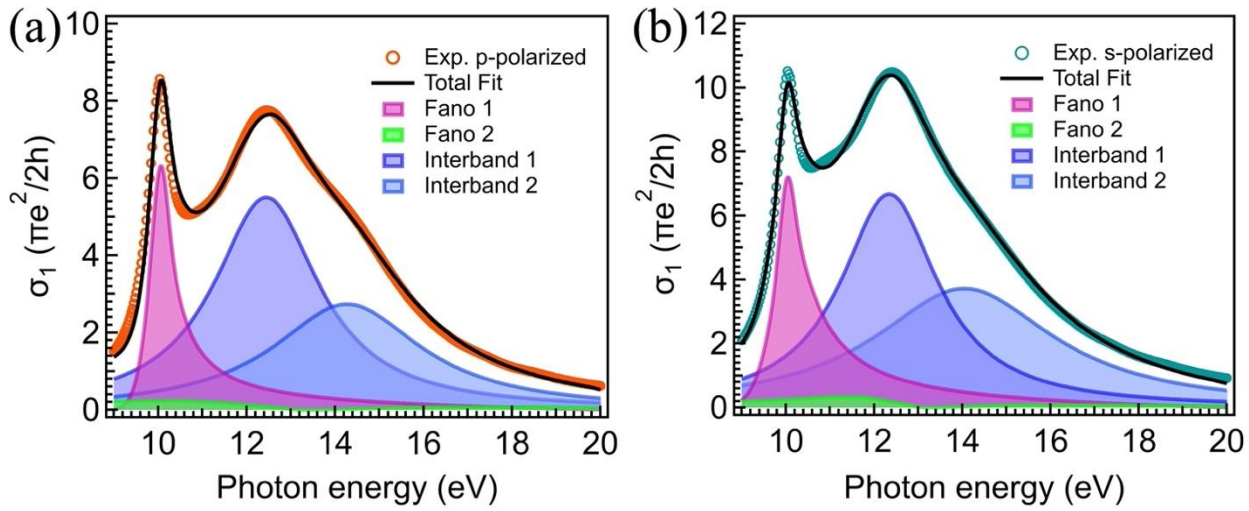

FIG. 4. Decomposition of the room-temperature optical conductivity of single-layer graphene: (a) p-polarized and (b) s-polarized. The black curve represents the overall spectrum fit with two Fano resonances (purple and green) and two interband transitions (blue).

The presence of this Fano resonance can be described by the formula [26]: $\sigma_1/\sigma_{1,\mathrm{cont}} = (q+\varepsilon)^2/1+\varepsilon^2$, where $\sigma_{1,\mathrm{cont}}$ represents the continuum contribution to σ_1, possibly affected by e–e interactions, and $\varepsilon = 2(\omega - E_{res})/\Gamma$, where Γ is the lifetime-related width of an exciton, and E_{res} is the resonance energy. The line shape is determined by the numbers q and q^2 is the ratio of the intensity of the excitonic transition to the unperturbed band-to-band transition.

Figure 4 (a-b) display the best fit of σ_1 for s- and p-polarizations using the Fano analysis and Lorentz model, with the parameters tabulated in Table S1 in Ref. [13]. The optical conductivity spectrum displays a unique double-peak behavior due to the comparable optical absorption of both excitons. This differs from the spectra of bulk metals, 1-D metallic carbon nanotubes [57–59], and semiconductors, where excitons either thoroughly wash out the absorption spectrum [60], remain unchanged, or are dominated by resonant excitons [61]. Conventionally, low-energy excitonic effects (electron-hole interactions) are important in determining the optical responses of semiconductors and associated renewable energy applications. In conventional semiconductors such as Si, the binding energy of bound exciton is ~10 meV binding energy, which has a lifetime of ~6.6 ns. While, in graphene, we estimate that the binding energy and the lifetime of resonant exciton at ~10.04 eV are ~100 meV and ~65.8 ns (from the Fano model). These resonant exciton binding energy and its lifetime are significantly larger and longer than Si semiconductors. Based on GW-BSE [17], the calculated binding energy of resonant exciton in graphene is ~270 meV, which is close to our experimental data. While the binding energy of the low-energy resonant exciton for metallic CNTs is ~30-50 meV [58–60].

In conclusion, we observe novel room temperature soft X-ray 2D correlated-plasmons with extremely low-plasmonic-loss and high-optical-energy resonant excitons in graphene. These optical properties are 2D nature of graphene and occur due to electron-electron and electron-hole

interactions. Our result calls for further investigations of high-energy optics and electronic correlation in graphene and 2D semimetals as correlated electron systems and opens new opportunities in optoelectronic applications by utilizing high-energy optical properties of 2D semimetals.

This work was supported by "Hibah Kerjasama Luar Negeri dan Publikasi Internasional (KLN), DPRM–Kemenristekdikti 2016, Indonesia" and the "International Centre for Theoretical Physics (ICTP)–ELETTRA User Programme 2015". The experiments at BEAR beamline-ELETTRA (Trieste, Italy) were conducted under the proposal 20155463. The work at the National University of Singapore was supported by the Ministry of Education of Singapore (MOE) AcRF Tier-2 (MOE-T2EP50220-0018 and T2EP50122-0028).

[1] H. Eskes, M. B. J. Meinders, and G. A. Sawatzky, *Anomalous Transfer of Spectral Weight in Doped Strongly Correlated Systems*, Phys Rev Lett **67**, 1035 (1991).
[2] A. Rusydi et al., *Metal-Insulator Transition in Manganites: Changes in Optical Conductivity up to 22 EV*, Phys Rev B Condens Matter Mater Phys **78**, 125110 (2008).
[3] P. Phillips, *Colloquium: Identifying the Propagating Charge Modes in Doped Mott Insulators*, Rev Mod Phys **82**, 1719 (2010).
[4] T. J. Whitcher et al., *Unravelling Strong Electronic Interlayer and Intralayer Correlations in a Transition Metal Dichalcogenide*, Nat Commun **12**, 6980 (2021).
[5] A. K. Geim and K. S. Novoselov, *The Rise of Graphene*, Nat Mater **6**, 183 (2007).
[6] A. H. Castro Neto, F. Guinea, N. M. R. Peres, K. S. Novoselov, and A. K. Geim, *The Electronic Properties of Graphene*, Rev Mod Phys **81**, 109 (2009).
[7] D. A. Bandurin, A. Principi, I. Y. Phinney, T. Taniguchi, K. Watanabe, and P. Jarillo-Herrero, *Interlayer Electron-Hole Friction in Tunable Twisted Bilayer Graphene Semimetal*, Phys Rev Lett **129**, 206802 (2022).
[8] D. N. Basov, M. M. Fogler, A. Lanzara, F. Wang, and Y. Zhang, *Colloquium: Graphene Spectroscopy*, Rev Mod Phys **86**, 959 (2014).
[9] T. C. Asmara et al., *Tunable and Low-Loss Correlated Plasmons in Mott-like Insulating Oxides*, Nat Commun **8**, 15271 (2017).
[10] H. Katow, R. Akashi, Y. Miyamoto, and S. Tsuneyuki, *First-Principles Study of the Optical Dipole Trap for Two-Dimensional Excitons in Graphane*, Phys Rev Lett **129**, 047401 (2022).
[11] I. Santoso et al., *Observation of Room-Temperature High-Energy Resonant Excitonic Effects in Graphene*, Phys Rev B Condens Matter Mater Phys **84**, 081403(R) (2011).

[12] K. F. Mak, L. Ju, F. Wang, and T. F. Heinz, *Optical Spectroscopy of Graphene: From the Far Infrared to the Ultraviolet*, Solid State Commun **152**, 1341 (2012).
[13] See Supplemental Material for more details on analysis of reflectivity, loss function and optical conductivity
[14] L. Yang, J. Deslippe, C. H. Park, M. L. Cohen, and S. G. Louie, *Excitonic Effects on the Optical Response of Graphene and Bilayer Graphene*, Phys Rev Lett **103**, 186802 (2009).
[15] P. E. Trevisanutto, M. Holzmann, M. Côté, and V. Olevano, *Ab Initio High-Energy Excitonic Effects in Graphite and Graphene*, Phys Rev B Condens Matter Mater Phys **81**, 121405(R) (2010).
[16] L. Yang, *Excitonic Effects on Optical Absorption Spectra of Doped Graphene*, Nano Lett **11**, 3844 (2011).
[17] L. Yang, *Excitons in Intrinsic and Bilayer Graphene*, Phys Rev B Condens Matter Mater Phys **83**, 085405 (2011).
[18] P. K. Gogoi, I. Santoso, S. Saha, S. Wang, A. H. C. Neto, K. P. Loh, T. Venkatesan, and A. Rusydi, *Optical Conductivity Study of Screening of Many-Body Effects in Graphene Interfaces*, Europhysics Letter **99**(6), 67009 (2012).
[19] Y. C. Chang, C. H. Liu, C. H. Liu, Z. Zhong, and T. B. Norris, *Extracting the Complex Optical Conductivity of Mono- and Bilayer Graphene by Ellipsometry*, Appl Phys Lett **104**, 261909 (2014).
[20] K. K. Tikuišis, A. Dubroka, K. Uhlířová, F. Speck, T. Seyller, M. Losurdo, M. Orlita, and M. Veis, *Dielectric Function of Epitaxial Quasi-Freestanding Monolayer Graphene on Si-Face 6H-SiC in a Broad Spectral Range*, Phys Rev Mater **7**, 044201 (2023).
[21] A. N. Toksumakov et al., *Anomalous Optical Response of Graphene on Hexagonal Boron Nitride Substrates*, Commun Phys **6**, 13 (2023).
[22] W. Li, G. Cheng, Y. Liang, B. Tian, X. Liang, L. Peng, A. R. Hight Walker, D. J. Gundlach, and N. V. Nguyen, *Broadband Optical Properties of Graphene by Spectroscopic Ellipsometry*, Carbon N Y **99**, 348 (2016).
[23] V. G. Kravets, A. N. Grigorenko, R. R. Nair, P. Blake, S. Anissimova, K. S. Novoselov, and A. K. Geim, *Spectroscopic Ellipsometry of Graphene and an Exciton-Shifted van Hove Peak in Absorption*, Phys Rev B Condens Matter Mater Phys **81**, 155413 (2010).
[24] G. Isić, *Spectroscopic Ellipsometry of Few-Layer Graphene*, J Nanophotonics **5**, 051809 (2011).
[25] A. Matković, U. Ralević, G. Isić, M. M. Jakovljević, B. Vasić, I. Milošević, D. Marković, and R. Gajić, *Spectroscopic Ellipsometry and the Fano Resonance Modeling of Graphene Optical Parameters*, Phys Scr **T149**, 014069 (2012).
[26] K. F. Mak, J. Shan, and T. F. Heinz, *Seeing Many-Body Effects in Single- and Few-Layer Graphene: Observation of Two-Dimensional Saddle-Point Excitons*, Phys Rev Lett **106**, 046401 (2011).
[27] J. W. Weber, V. E. Calado, and M. C. M. Van De Sanden, *Optical Constants of Graphene Measured by Spectroscopic Ellipsometry*, Appl Phys Lett **97**, 091904 (2010).
[28] F. J. Nelson, V. K. Kamineni, T. Zhang, E. S. Comfort, J. U. Lee, and A. C. Diebold, *Optical Properties of Large-Area Polycrystalline Chemical Vapor Deposited Graphene by Spectroscopic Ellipsometry*, Appl Phys Lett **97**, 253110 (2010).
[29] K. F. Mak, M. Y. Sfeir, Y. Wu, C. H. Lui, J. A. Misewich, and T. F. Heinz, *Measurement of the Optical Conductivity of Graphene*, Phys Rev Lett **101**, 196405 (2008).

[30] T. Kobayashi et al., *Production of a 100-m-Long High-Quality Graphene Transparent Conductive Film by Roll-to-Roll Chemical Vapor Deposition and Transfer Process*, Appl Phys Lett **102**, 023112 (2013).
[31] S. Zhang, Z. Li, and F. Xing, *Review of Polarization Optical Devices Based on Graphene Materials*, Int J Mol Sci **21**, 1608 (2020).
[32] Y. Zhang, Y. Feng, B. Zhu, J. Zhao, and T. Jiang, *Graphene Based Tunable Metamaterial Absorber and Polarization Modulation in Terahertz Frequency*, Opt Express **22**, 22743 (2014).
[33] Q. Bao, H. Zhang, B. Wang, Z. Ni, C. H. Y. X. Lim, Y. Wang, D. Y. Tang, and K. P. Loh, *Broadband Graphene Polarizer*, Nat Photonics **5**, 411 (2011).
[34] M. Liu, X. Yin, E. Ulin-Avila, B. Geng, T. Zentgraf, L. Ju, F. Wang, and X. Zhang, *A Graphene-Based Broadband Optical Modulator*, Nature **474**, 64 (2011).
[35] T. Mueller, F. Xia, and P. Avouris, *Graphene Photodetectors for High-Speed Optical Communications*, Nat Photonics **4**, 297 (2010).
[36] R. Hao, W. Du, H. Chen, X. Jin, L. Yang, and E. Li, *Ultra-Compact Optical Modulator by Graphene Induced Electro-Refraction Effect*, Appl Phys Lett **103**, 061116 (2013).
[37] Q. Ye, J. Wang, Z. Liu, Z.-C. Deng, X.-T. Kong, F. Xing, X.-D. Chen, W.-Y. Zhou, C.-P. Zhang, and J.-G. Tian, *Polarization-Dependent Optical Absorption of Graphene under Total Internal Reflection*, Appl Phys Lett **102**, 021912 (2013).
[38] J. Yang, D. Chen, J. Zhang, Z. Zhang, and J. Huang, *Polarization Modulation Based on the Hybrid Waveguide of Graphene Sandwiched Structure*, EPL (Europhysics Letters) **119**, 54001 (2017).
[39] R. Wang, D. Li, H. Wu, M. Jiang, Z. Sun, Y. Tian, J. Bai, and Z. Ren, *All-Optical Intensity Modulator by Polarization-Dependent Graphene-Microfiber Waveguide*, IEEE Photonics J **9**, 7105708 (2017).
[40] N. A. Malik, P. Nicolosi, K. Jimenez, A. Gaballah, A. Giglia, M. Lazzarino, and P. Zuppella, *Experimental Study of Few-Layer Graphene: Optical Anisotropy and Pseudo-Brewster Angle Shift in Vacuum Ultraviolet Spectral Range*, Adv Photonics Res **2**, 2000207 (2021).
[41] A. Matković, U. Ralević, M. Chhikara, M. M. Jakovljević, D. Jovanović, G. Bratina, and R. Gajić, *Influence of Transfer Residue on the Optical Properties of Chemical Vapor Deposited Graphene Investigated through Spectroscopic Ellipsometry*, J Appl Phys **114**, 093505 (2013).
[42] M. Houmad, H. Zaari, A. Benyoussef, A. El Kenz, and H. Ez-Zahraouy, *Optical Conductivity Enhancement and Band Gap Opening with Silicon Doped Graphene*, Carbon N Y **94**, 1021 (2015).
[43] M. A. El-Sayed et al., *Optical Constants of Chemical Vapor Deposited Graphene for Photonic Applications*, Nanomaterials **11**, 1230 (2021).
[44] Y. Y. Wang, Z. H. Ni, T. Yu, Z. X. Shen, H. M. Wang, Y. H. Wu, W. Chen, and A. T. S. Wee, *Raman Studies of Monolayer Graphene: The Substrate Effect*, Journal of Physical Chemistry C **112**, 10637 (2008).
[45] C. Jia, J. Jiang, L. Gan, and X. Guo, *Direct Optical Characterization of Graphene Growth and Domains on Growth Substrates*, Sci Rep **2**, 707 (2012).
[46] J. Hass, F. Varchon, J. E. Millán-Otoya, M. Sprinkle, N. Sharma, W. A. De Heer, C. Berger, P. N. First, L. Magaud, and E. H. Conrad, *Why Multilayer Graphene on 4H-SiC(000$\bar{1}$) Behaves like a Single Sheet of Graphene*, Phys Rev Lett **100**, 125504 (2008).

[47] W. Zhu, V. Perebeinos, M. Freitag, and P. Avouris, *Carrier Scattering, Mobilities, and Electrostatic Potential in Monolayer, Bilayer, and Trilayer Graphene*, Phys Rev B **80**, 235402 (2009).
[48] E. H. Hwang, S. Adam, and S. Das Sarma, *Carrier Transport in Two-Dimensional Graphene Layers*, Phys Rev Lett **98**, 186806 (2007).
[49] S. Nannarone, *The BEAR Beamline at Elettra*, in *AIP Conference Proceedings*, Vol. 705, pp. 450–453 (2004).
[50] T. C. Asmara et al., *Mechanisms of Charge Transfer and Redistribution in $LaAlO_3/SrTiO_3$ Revealed by High-Energy Optical Conductivity*, Nat Commun **5**, 3663 (2014).
[51] T. C. Asmara, I. Santoso, and A. Rusydi, *Self-Consistent Iteration Procedure in Analyzing Reflectivity and Spectroscopic Ellipsometry Data of Multilayered Materials and Their Interfaces*, Review of Scientific Instruments **85**, 123116 (2014).
[52] I. Santoso, S. L. Wong, X. Yin, P. K. Gogoi, T. C. Asmara, H. Huang, W. Chen, A. T. S. Wee, and A. Rusydi, *Optical and Electronic Structure of Quasi-Freestanding Multilayer Graphene on the Carbon Face of SiC*, EPL **108**, 37009 (2014).
[53] W. Li, G. Cheng, Y. Liang, B. Tian, X. Liang, L. Peng, A. R. Hight Walker, D. J. Gundlach, and N. V. Nguyen, *Broadband Optical Properties of Graphene by Spectroscopic Ellipsometry*, Carbon N Y **99**, 348 (2016).
[54] T. Andreescu, C. Mortici, and M. Tetiva, *Mathematical Bridges* (Springer New York, 2017).
[55] Y. W. Sun, D. Holec, D. Gehringer, L. Li, O. Fenwick, D. J. Dunstan, and C. J. Humphreys, *Graphene on Silicon: Effects of the Silicon Surface Orientation on the Work Function and Carrier Density of Graphene*, Phys Rev B **105**, 165416 (2022).
[56] U. Fano, *Effects of Configuration Interaction on Intensities and Phase Shifts*, Physical Review **124**, 1866 (1961).
[57] L. Fleming, M. D. Ulrich, K. Efimenko, J. Genzer, A. S. Y. Chan, T. E. Madey, S.-J. Oh, O. Zhou, and J. E. Rowe, *Near-Edge Absorption Fine Structure and UV Photoemission Spectroscopy Studies of Aligned Single-Walled Carbon Nanotubes on Si(100) Substrates*, Journal of Vacuum Science & Technology B: Microelectronics and Nanometer Structures Processing, Measurement, and Phenomena **22**, 2000 (2004).
[58] C. D. Spataru, S. Ismail-Beigi, L. X. Benedict, and S. G. Louie, *Excitonic Effects and Optical Spectra of Single-Walled Carbon Nanotubes*, Phys Rev Lett **92**, 7 (2004).
[59] F. Wang, D. J. Cho, B. Kessler, J. Deslippe, P. J. Schuck, S. G. Louie, A. Zettl, T. F. Heinz, and Y. R. Shen, *Observation of Excitons in One-Dimensional Metallic Single-Walled Carbon Nanotubes*, Phys Rev Lett **99**, 227401 (2007).
[60] J. Deslippe, C. D. Spataru, D. Prendergast, and S. G. Louie, *Bound Excitons in Metallic Single-Walled Carbon Nanotubes*, Nano Lett **7**, 1626 (2007).
[61] M. Rohlfing and S. G. Louie, *Electron-Hole Excitations and Optical Spectra from First Principles*, Phys Rev B **62**, 4927 (2000).